PHYSICAL REVIEW B VOLUME 24, NUMBER 2 15 JULY 1981

# Dielectric band structure of crystals: General properties and calculations for silicon

R. Car*
*Scuola Internazionale Superiore di Studi Avanzati, Trieste, Italy*
*and Laboratoire de Physique Experimentale, Ecole Polytechnique Federale, Lausanne, Switzerland†*

E. Tosatti
*Gruppo Nazionale di Struttura della Materia, Istituto di Fisica Teorica, Universitá di Trieste, Trieste, Italy*
*Scuola Internazionale Superiore di Studi Avanzati, Trieste, Italy,*
*and International Center for Theoretical Physics, Trieste, Italy*

S. Baroni
*Laboratoire de Physique Theorique, Ecole Polytechnique Federale, Lausanne, Switzerland*

S. Leelaprute
*International Center for Theoretical Physics, Trieste, Italy*
*and Scuola Internazionale Superiore di Studi Avanzati, Trieste, Italy*

(Received 9 March 1981)

We develop the dielectric band-structure method, originally proposed by Baldereschi and Tosatti, for the description of microscopic electronic screening in crystals. Some general properties are examined first, including the requirements of causality and stability. The specific test case of silicon is then considered. Dielectric bands are calculated, according to several different prescriptions for the construction of the dielectric matrix. It is shown that the results allow a very direct appraisal of the screening properties of the system, as well as of the quality of the dielectric model adopted. The electronic charge displacement induced by $\Gamma_{25}'$ and $X_3$ phononlike displacements of the atoms is also calculated and compared with the results of existent fully self-consistent calculations. Conclusions are drawn on the relative accuracies of the dielectric band structures.

## I. INTRODUCTION

The study of electronic dielectric properties of crystals including local fields implies the use of dielectric matrices (DM).[1,2] The calculation of these matrices starting from realistic band structures has proven to be extremely elaborate, even if a great simplication can be introduced by using, e.g., the mean-value point technique and its extensions[3] or other techniques.[4] Such accurate DM calculations are available for a few materials only.[5-11] Furthermore, most numerical results are only available in the $\vec{q} \to 0$ limit.

Various models have been proposed to simplify the task of calculating the full DM at all $\vec{q}$ vectors. These models are generally based on simplified electronic band structures[12-17] and/or on other more or less reasonable assumptions on the structure of the DM.[18-21] The relative accuracy of the different models has not yet been established. On the other hand, the development of reliable simple static DM models is absolutely vital to future important applications such as phonon calculations, screening of defects, local-field calculations in real space, etc. If this is true for those few materials where a great deal is already known at $\vec{q} \to 0$, the need is even more evident for the infinite variety of other crystals where one hardly knows anything other than the static $\vec{q} = 0$ dielectric constant.

Baldereschi and Tosatti have recently proposed a "dielectric band-structure" (DBS) scheme,[22] whereby the static ($\omega = 0$) DM is diagonalized, yielding screening eigenvalues and eigenvectors for each $\vec{q}$ in the Brillouin zone (BZ). They have shown that in this way symmetry emerges naturally in the screening problem and that the information contents of the full DM, a very large matrix, is cast into very few eigenvalues and eigenvectors for each symmetry.

In this paper, we (a) clarify further some general properties of the dielectric band-structure approach, (b) present explicit calculations for the DBS of Si throughout the Brillouin zone, and (c) compare qualities and defects of different available DM models, by direct calculation of their DBS, as well as of the screening charge induced by some high-symmetry phononlike displacements of the atoms.

The main point of general nature which apparently has not received proper attention thus far concerns the restrictions which causality on one hand and thermodynamic stability on the other hand impose on any given DM. We show that the dielectric band-structure formulation is a very natural one for stating clearly these requirements, thus extending all the very-well-known properties of diagonal response functions $\epsilon(\vec{q}, \omega)$ to the more complicated nonlocal response matrix $\epsilon(\vec{q}+\vec{G}, \vec{q}+\vec{G}', \omega)$ typical of all inhomogeneous systems. This line is developed in Sec. II.

Calculating the dielectric band structure out of

 

a given DM model—there is a variety of such models in the field—turns out to be a rather stringent and instructive test. In Sec. III we describe some of these models, including one very newly developed, based on the density-functional formulation. A brief derivation of this model is sketched in the Appendix A. The dielectric band structures for all these models are then presented and discussed in Sec. IV.

A certain class of models, namely, those based on the "factorization ansatz," which has been proposed for extreme tight-binding situations, turns out to have surprisingly few dielectric bands. As is shown in Appendix B, this is a general consequence of the factorizable form of these dielectric matrices. The obvious consequence is that only problems which involve the limited set of symmetries represented by these few bands can be handled with such matrices.

As a realistic application which allows a further comparison between various screening models, we present in Sec. V a calculation of the electron charge density induced by a phononlike displacement of the Si atoms. This calculation is particularly informative, since the same quantity has also been computed by an accurate self-consistent pseudopotential method by Baldereschi and Maschke.[23] The general conclusions that this type of comparison allows are very close to those drawn by just looking at the DBS of the different models. This lends further support to the validity of the dielectric band structure method.

## II. GENERAL PROPERTIES

The exact inverse longitudinal DM of a general many-body system with crystalline translational properties is given by[1]

$$\epsilon^{-1}(\vec{q}+\vec{G},\vec{q}+\vec{G}',\omega)=\delta_{\vec{G}\vec{G}'}-v(\vec{q}+\vec{G})\chi(\vec{q}+\vec{G},\vec{q}+G',\omega)\,, \tag{2.1}$$

with

$$\chi(\vec{q}+\vec{G},\vec{q}+\vec{G}',\omega)=\sum_n \langle 0|\hat{\rho}^{*}_{\vec{q}+\vec{G}}|n\rangle\langle n|\hat{\rho}_{\vec{q}+\vec{G}'}|0\rangle D_{n0}(\omega)\,,$$

$$D_{n0}(\omega)=(E_n-E_0+\omega+i0^+)^{-1}+(E_n-E_0-\omega-i0^+)^{-1}\,,$$

$$\hat{\rho}_{\vec{q}+\vec{G}}=\sum_l \exp[i(\vec{q}+\vec{G})\cdot\vec{r}_l]\,,$$

where $v(Q)=4\pi e^2/Q^2\Omega$, $l$ runs over all electrons, $|0\rangle, E_0$ and $|n\rangle, E_n$ denote exact ground-state and excited-state eigenvectors and energies, $\vec{G}$ denotes a reciprocal-lattice vector, and $\vec{q}$ is the wave vector inside the BZ. The existence of nonzero off-diagonal elements, $\vec{G}\neq\vec{G}'$, is connected with spatial inhomogeneity of the electrons, caused by the periodic lattice potential.

At $\omega=0$, the matrix $\chi(\vec{q}+\vec{G},\vec{q}+\vec{G}')$ becomes Hermitian, but the DM $\epsilon(\vec{q}+\vec{G},\vec{q}+\vec{G}')$ does not, due to the presence of the prefactor $v(\vec{q}+\vec{G})$. Yet the DM can be diagonalized with real eigenvalues. This is seen by first defining a Hermitian $\tilde{\epsilon}^{-1}$ in the form

$$\tilde{\epsilon}^{-1}(\vec{q}+\vec{G},\vec{q}+\vec{G}')=\left(\frac{v(\vec{q}+\vec{G}')}{v(\vec{q}+\vec{G})}\right)^{1/2}\epsilon^{-1}(\vec{q}+\vec{G},\vec{q}+\vec{G}')\,. \tag{2.2}$$

Once this $\tilde{\epsilon}^{-1}$ is diagonalized with eigenvalues $\tilde{\epsilon}^{-1}_{\nu}(\vec{q})$ and Bloch-type eigenvectors

$$\tilde{\phi}^{\nu}_{\vec{q}}(\vec{r})=e^{i\vec{q}\cdot\vec{r}}\sum_{\vec{G}} C^{\nu}_{\vec{G}}(\vec{q})e^{i\vec{G}\cdot\vec{r}}\,, \tag{2.3}$$

it is easily verified that

$$\epsilon^{-1}_{\nu}(\vec{q})=\tilde{\epsilon}^{-1}_{\nu}(\vec{q}) \tag{2.4}$$

and

$$\phi^{\nu}_{q}(\vec{r})=e^{i\vec{q}\cdot\vec{r}}\sum_{\vec{G}}[v(q+G)]^{1/2}C^{\nu}_{\vec{G}}(\vec{q})e^{i\vec{G}\cdot\vec{r}} \tag{2.5}$$

are eigenvalues and eigenvectors of the DM itself. This is the dielectric band-structure (DBS) scheme.[22]

Some properties of the DBS of crystals have already been discussed.[22] In this section we extend this discussion, mainly to include causality properties.

In the homogeneous case, it is well known that $1/\epsilon(\vec{q},\omega)$ is a causal response function for all values of $\vec{q}$, while the same is not true of $\epsilon(\vec{q},\omega)$ itself.[24,25] The reason is that while $1/\epsilon(\vec{q},\omega)$ describes the response to an external field, $\epsilon(\vec{q},\omega)$ is instead the response to the internal field, which cannot be varied at will, but depends itself on the response of the medium. Kirzhnits[25] has shown that only in the macroscopic limit, $\vec{q}\to 0$, the dielectric function $\epsilon(\vec{q},\omega)$ becomes itself a causal response function. Thus the Kramers-Kronig relations, which hold for $\epsilon^{-1}(\vec{q},\omega)$ at all wavelengths, become valid also for $\epsilon(\vec{q},\omega)$ only in the $\vec{q}\to 0$ limit:

$$\mathrm{Re}\epsilon^{-1}(\vec{q},\omega)=1+\frac{2}{\pi}\,\mathrm{P}\int_0^{\infty}\frac{\omega'\,\mathrm{Im}\epsilon^{-1}(\vec{q},\omega)}{\omega'^2-\omega^2}\,d\omega'\,, \tag{2.6a}$$

$$\mathrm{Re}\epsilon(0,\omega)=1+\frac{2}{\pi}\,\mathrm{P}\int_0^{\infty}\frac{\omega'\,\mathrm{Im}\epsilon(0,\omega)}{\omega'^2-\omega^2}\,d\omega'\,. \tag{2.6b}$$

Introducing the important fact that a system at thermodynamic equilibrium can only absorb energy at any given positive frequency, which implies $\mathrm{Im}\epsilon^{-1}(\vec{q},\omega)<0$, $\mathrm{Im}\epsilon(0,\omega)>0$, and specializing (2.6) for $\omega=0$, one gets that for a stable system

$$1/\epsilon(\vec{q},0)<1 \tag{2.7}$$

for all $\vec{q}$, while for $\vec{q}\to 0$

$$\epsilon_0=\lim_{\vec{q}\to 0}\epsilon(\vec{q},0)>1 \tag{2.8}$$

must also hold. Therefore, a system is unstable if either $\epsilon^{-1}(\vec{q},0)\geq 1$ or $\epsilon^{-1}(\vec{q},0)\leq 0$ for $\vec{q}\to 0$. However, at finite $\vec{q}$, only $\epsilon^{-1}(\vec{q},0)\geq 1$ involves instability, while $\epsilon^{-1}(\vec{q},0)\leq 0$ is perfectly allowed.[25] Systems with negative ionic dielectric function $\epsilon(\vec{q},0)$ can be found experimentally.[26] No system with negative *electronic* $\epsilon(\vec{q},0)$ appears to have been explicitly discussed, but some must surely exist. Good candidates should be systems at temperatures just above electronic superlattice phase transitions, like for example charge-density waves or Wigner transitions. In fact, a transition of this type, if continuous, must be signaled by

$$\epsilon^{-1}(\vec{q},0)\xrightarrow[T=T_c]{}-\infty,$$

as discussed later in this section. Just above $T_c$, $\epsilon^{-1}(\vec{q},0)$ should rise continuously from $-\infty$ towards zero, to become eventually positive only when, sufficiently away from $T_c$, the critical fluctuations are dying out.

We note, in passing, that the well-known one-electron, or random-phase approximation (RPA), for the electronic response of a crystal[27] always yields a causal $\epsilon(\vec{q},\omega)$ rather than a causal $\epsilon^{-1}(\vec{q},\omega)$. Specifically

$$\epsilon^{\mathrm{RPA}}(\vec{q},0)=1+2v(q)\sum_{\vec{k},v,c}\frac{|\langle v\vec{k}|e^{-i\vec{q}\cdot\vec{r}}|c\vec{k}+\vec{q}\rangle|^2}{E_c(\vec{k}+\vec{q})-E_v(\vec{k})}, \tag{2.9}$$

which is larger than one for all $q$, since by definition conduction states $E_c$ lie above valence states $E_v$. Therefore, the occurrence of a negative electronic $\epsilon(q,0)$, which is in general possible, must be necessarily due to so-called exchange and correlation effects, not contained in the RPA.

The natural question at this point is: How do these properties change in passing from homogeneous systems, characterized by a dielectric function $\epsilon^{-1}(\vec{q},\omega)$, to an inhomogeneous system, particularly a crystal, characterized by a DM $\epsilon^{-1}(\vec{q}+\vec{G},\vec{q}+\vec{G}',\omega)$? As it turns out, the DBS scheme provides a very natural way to answer this question. The equivalent of (2.7) is that all dielectric eigenvalues must be smaller than unity,

$$\epsilon_\nu^{-1}(\vec{q})<1. \tag{2.10}$$

The proof is as follows. The dielectric eigenvalues $\epsilon_\nu^{-1}(\vec{q})$ can be seen as expectation values of an operator $\epsilon_{\mathrm{op}}^{-1}$, between eigenpotentials

$$\epsilon_\nu^{-1}(\vec{q})=\langle\phi_{\vec{q}}^\nu|\epsilon_{\mathrm{op}}^{-1}|\phi_{\vec{q}}^\nu\rangle=\langle\tilde{\phi}_{\vec{q}}^\nu|\tilde{\epsilon}_{\mathrm{op}}^{-1}|\tilde{\phi}_{\vec{q}}^\nu\rangle=\delta_{\nu\nu'}\left(1-\frac{4\pi e^2}{\Omega}\sum_{\vec{G}\vec{G}'}\frac{C_{\vec{G}}^\nu(\vec{q})C_{\vec{G}'}^{*\nu'}(\vec{q})}{|\vec{q}+\vec{G}||\vec{q}+\vec{G}'|}\chi(\vec{q}+\vec{G},\vec{q}+\vec{G}',0)\right), \tag{2.11}$$

where use has been made of (2.3) and (2.1). The second term in parentheses can also be written as

$$\frac{8\pi e^2}{\Omega}\sum_{n\neq 0}(E_n-E_0)^{-1}\left|\sum_{\vec{G}}C_{\vec{G}}^\nu(\vec{q})|\vec{q}+\vec{G}|^{-1}\langle 0|\hat{\rho}_{\vec{q}+\vec{G}}^*|n\rangle\right|^2, \tag{2.12}$$

and is always positive, since $E_n>E_0$. Hence (2.10) is proved.

Having found the extension of (2.7) in (2.10), we can now look for the extension of (2.8) to the crystalline case. The macroscopic dielectric function is well known to be[2]

$$\epsilon_0=\lim_{\vec{q}\to 0}1/\epsilon^{-1}(\vec{q},\vec{q},0), \tag{2.13}$$

whence, by repeating Kirzhnits's arguments,[25] (2.8) is here replaced by

$$\lim_{\vec{q}\to 0}1/\epsilon^{-1}(\vec{q},\vec{q},0)>1. \tag{2.14}$$

This is not an obvious condition to be verified on any single eigenvalue of the DM, for $\vec{q}\to 0$. This is because in the crystal, $e^{i\vec{q}\cdot\vec{r}}$ is not an eigenpotential, but can only be expressed as a sum of eigenpotentials

$$\exp(i\vec{q}\cdot\vec{r})=\sum_\nu a_{\vec{q}}^\nu\phi_{\vec{q}}^\nu(\vec{r}). \tag{2.15}$$

Then, the inequality (2.14), which is the crystal generalization of (2.8), is only a weak condition on the eigenvalues

$$\lim_{\vec{q}\to 0}\left(\sum_\nu|a_{\vec{q}}^\nu|^2\epsilon_\nu^{-1}(\vec{q})\right)^{-1}>1. \tag{2.16}$$

The two inequalities (2.10) and (2.16) must be satisfied by any DBS for $\vec{q}\to 0$, while for a general $\vec{q}$ in the BZ only (2.10) holds. Again, in passing, we note that in the RPA the exact (2.10) is replaced by

$$\epsilon_\nu^{\mathrm{RPA}}(\vec{q})>1$$

which coincides with (2.10) only as long as $\epsilon_\nu^{-1}(\vec{q})\geq 0$.

We can now extend the condition for thermodynamic instability discussed previously to the inhomogeneous crystalline case. By virtue of (2.10), any value of $\epsilon_\nu^{-1}(\vec{q})$ between 1 and $-\infty$ is compatible with stability. At $\vec{q}\to 0$, (2.16) must also be obeyed. A negative dielectric eigenvalue

simply means that a particular perturbation equal to the corresponding eigenpotential is overscreened. Overscreening at some special sites is possible even in the RPA. For instance, in the case of Si, an external uniform field (which is, of course, not an eigenpotential) is overscreened in a small volume centered at the bond sites.[28]

A crystal is unstable when any of the $\epsilon_\nu^{-1}(\vec{q})$ is $\geq 1$. It is clear that if a system is to approach instability in a continuous fashion this can only occur with at least one of the eigenvalues crossing over to $-\infty$:

$$\epsilon_\nu^{-1}(\vec{q}) \to -\infty . \tag{2.17}$$

Inspection of (2.11) shows that this will occur when at least one excited state of the crystal becomes degenerate with the ground state

$$E_n - E_0 \to 0 . \tag{2.18}$$

A well-known example of this behavior is the occurrence of soft lattice modes in ferroelectric and antiferroelectric phase transitions.[29] Its electronic equivalent, which is so far hypothetical, however, is a soft plasmon[30] or exciton[31] mode in charge-density-wave transitions. The obvious implication of the equivalence between (2.17) and (2.18) is that the order parameter for a continuous electronic phase transition in a crystal *must be* a dielectric eigenstate.

Armed with this summary of the requisites that any DM must satisfy if it is to describe a causal and stable crystal, we can now move on to consider specific DM models.

## III. MODELS FOR STATIC DIELECTRIC SCREENING IN Si

We give in this section a brief description of the various DM models whose DBS's will be discussed in this paper. Among several possibilities, we have chosen as illustrative examples the models of Sinha,[18,19] of Johnson,[20] of Car and Selloni,[21] and a newly developed one based on the local-density-functional formulation.[32]

### A. Sinha model

We consider only a particular form of the Sinha model which gives rise to the so-called generalized shell model, when applied to lattice dynamics calculations.[18] In this model the DM is assumed to have the following factorizable form:

$$\epsilon(\vec{q}+\vec{G},\vec{q}+\vec{G}') = \epsilon_0(\vec{q}+\vec{G})\delta_{GG'} + a_1 v'(\vec{q}+\vec{G}) \sum_s f_s^*(\vec{q}+\vec{G}) f_s(\vec{q}+\vec{G}')(\vec{q}+\vec{G})\cdot(\vec{q}+\vec{G}') \exp[i(\vec{G}-\vec{G}')\cdot\vec{r}_s'] , \tag{3.1}$$

where $\epsilon_0(\vec{q}+\vec{G})$ is an *ad hoc* function introduced in order to adjust the diagonal part of the DM (3.1) to the calculated values of Walter and Cohen,[33] further corrected by exchange,[19] the sum is over the sites in the unit cell, $a_1$ is an adjustable parameter, $f_s(\vec{q}+\vec{G})$ are spherical form factors defined in Refs. 18 and 19, and $v'(\vec{Q})$ is an effective electron-electron interaction[34] given by

$$v'(\vec{Q}) = v(\vec{Q})[1 - f_{xc}(\vec{Q})] , \tag{3.2}$$

where $v(\vec{Q})$ is the Coulomb potential and $f_{xc}(\vec{Q})$ allows approximately for exchange and correlation effects.[35] In our application we use Eq. (3.1) with values of the parameter as appropriate for Si, given in Ref. 19.

It should be noted that form (3.1) is strictly justified only in the extreme tight-binding limit with flat bands.[36,37] Clearly a broad-band covalent crystal like Si is very far from this limit. Nevertheless, according to Sinha *et al.*[18,19] this model works fairly well, at least in lattice dynamics. A feature that makes this model attractive in spite of its crudeness is obviously its factorizable form that allows the DM to be inverted analytically to obtain $\epsilon^{-1}(\vec{q}+\vec{G},\vec{q}+\vec{G}')$, the quantity of physical importance.

### B. Johnson model

This model was constructed starting from a very different approach, i.e., from an off-diagonal generalization of the popular diagonal Penn model,[38] where an effectively one-dimensional gap is superposed to an otherwise free-electron model. In this sense Johnson's model is much more free-electron-like than Sinha's. Johnson's DM has the form

$$\epsilon(\vec{q}+\vec{G},\vec{q}+\vec{G}') = \delta_{\vec{G}\vec{G}'} + \frac{(\epsilon^{\mathrm{RPA}}-1)\rho(\vec{G}-\vec{G}')}{\{1+K[\vec{q}+\frac{1}{2}(\vec{G}+\vec{G}')]^2\}^2} \times \frac{(\vec{q}+\vec{G})\cdot(\vec{q}+\vec{G}')}{|\vec{q}+\vec{G}|^2} , \tag{3.3}$$

where $\epsilon^{\mathrm{RPA}}$ is the calculated $\epsilon(\vec{q},0)$ in the RPA, as computed, e.g., by Walter and Cohen,[33] $\rho(\vec{G})$ is the valence charge density that can be taken either from experiment or from empirical local pseudopotential band calculations,[39] and $K$ is a cutoff fixed by

Johnson as

$$K=\begin{cases}\hbar(\epsilon^{\mathrm{RPA}}-1)^{1/2}/2m\omega_p & \text{if } |\vec{G}-\vec{G}'|<2k_F\\ 0 & \text{if } |\vec{G}-\vec{G}'|>2k_F,\end{cases} \tag{3.4}$$

where $k_F$ is the Fermi momentum and $\omega_p=(4\pi ne^2/m)^{1/2}$. This cutoff, which is introduced rather arbitrarily, has the effect of seriously overestimating some off-diagonal matrix elements. For example, for small $\vec{q}$ and $|\vec{G}-\vec{G}'|>2k_F$ the cutoff may give rise to important nonzero off-diagonal DM elements even for very large $|\vec{G}|$ and $|\vec{G}'|$, which is unphysical since $\epsilon(\vec{q}+\vec{G},\vec{q}+\vec{G}')$ should go to zero at least as $O(G^{-4})$ for large $\vec{G}$ and $\vec{G}'=\vec{G}+\vec{\kappa}$, where $\kappa$ is a constant. Johnson's model was originally devised for diamond, giving quite good results for the DM elements in the limit $\vec{q}\to 0$, when compared with the accurate calculations of Van Vechten and Martin.[5] It is also rather simple and parameter-free, both the charge density $\rho(G)$ and $\epsilon_0$ being normally known. We did, however, get very poor results when we tried to apply this model to other semiconductors like Si or Ge.[40]

### C. Car-Selloni model

A modification of Johnson's model was introduced by Car and Selloni, who applied it to screening of point-charge impurities in Si.[21] In their model the DM takes the form

$$\epsilon(\vec{q},\vec{G},\vec{q}+\vec{G}')=f(\vec{q}+\vec{G})\delta_{\vec{G}\vec{G}'}+(1-\delta_{\vec{G}\vec{G}'})\frac{A\rho(\vec{G}-\vec{G}')}{[1+B|(\vec{q}+\vec{G})\cdot(\vec{q}+\vec{G}')|]^2}\frac{(\vec{q}+\vec{G})\cdot(\vec{q}+\vec{G}')}{|\vec{q}+\vec{G}|^2}\,. \tag{3.5}$$

Here the function $f(\vec{q}+\vec{G})$ is fitted to the diagonal dielectric function as calculated by Walter and Cohen,[33] and the constants $A$ and $B$ are adjusted to reproduce the off-diagonal DM elements as calculated in the limit $\vec{q}\to 0$ by Baldereschi and Tosatti,[11] and $\rho(\vec{G})$ is again that of Ref. 39.

The dielectric model (3.5) does not have the unphysical cutoff $K$ of the Johnson model. Its accuracy has been found to be nearly the same in various semiconductors.[40] However, unlike Johnson's model, this formulation depends upon the availability of accurate calculations of at least some off-diagonal DM elements (at $\vec{q}=0$, or elsewhere) so that the parameters $A$ and $B$ can be adjusted to fit them.

### D. Local-density model

A very simple dielectric matrix without adjustable parameters can be obtained from the local-density approximation of the density functional theory. The form we use here is

$$\epsilon(\vec{q}+\vec{G},\vec{q}+\vec{G}')=\delta_{GG'}-v(\vec{q}+\vec{G})R^{-1}(\vec{q}+\vec{G},\vec{q}+\vec{G}')\,, \tag{3.6}$$

where the matrix $R$ is given by

$$R(\vec{q}+\vec{G},\vec{q}+\vec{G}')=-\tfrac{10}{9}\,c_0(\rho^{-1/3})_{\vec{G}-\vec{G}'}-2\,c_1\left[[(\vec{q}+\vec{G})^2+(\vec{q}+\vec{G}')^2-(\vec{q}+\vec{G})\cdot(\vec{q}+\vec{G}')](\rho^{-1})_{\vec{G}-\vec{G}'}+\left(\frac{(\vec{\nabla}\rho)^2}{\rho^3}\right)_{\vec{G}-\vec{G}'}\right]. \tag{3.7}$$

Here $c_0=\frac{3}{10}(3\pi^2)^{2/3}$, $c_1=\frac{1}{72}$, $\rho$ is the valence charge density, and $(f(\vec{r}))_{\vec{G}}$ denotes the $\vec{G}$-Fourier transform of the function $f(\vec{r})$. The most important steps in the derivation of this model are sketched in Appendix A. For more details we refer to a future publication.[32]

Owing to the Thomas-Fermi form of the approximate functional (A1), the DM (3.6) has an undesired "metallic" behavior in the limit $\vec{q}\to 0$, that is, a $1/q^2$ divergence in $\epsilon(\vec{q},\vec{q})$ and $\epsilon(\vec{q},\vec{q}+\vec{G})$.[11] We expect, however, that except for these elements at $\vec{q}\to 0$, and generally for $\vec{q}\neq 0$, this model should constitute quite a reasonable approximation for a semiconductor DM. This can already be seen in the homogeneous approximation where the free-electron Lindhard or Thomas-Fermi dielectric function approaches rapidly the Penn dielectric function of a semiconductor of same average electron density, as soon as $|\vec{q}|$ is larger than a fraction of $k_{\mathrm{TF}}$.

## IV. DIELECTRIC BAND STRUCTURES FOR SILICON

We present in this section the results of the diagonalization of the different model DM's discussed in the preceding section. To provide a fixed reference point, we first reproduce from the work of Baldereschi and Tosatti[22] the "empty lattice" DBS obtained by simple folding of the inverse diagonal dielectric function $\epsilon^{-1}(\vec{q})$ without any off-diagonal elements. This is shown in Fig. 1. Also shown there is the result of an accurate diagonalization of the full DM calculated in the RPA and in the $\vec{q}\to 0$ limit only.[22] The shifts and splittings of these $\vec{q}=0$ dielectric eigenvalues with respect to the empty lattice DBS are indicative of

the effect of crystal inhomogeneity on screening, in the same way that the shifts and splittings in the electronic band structure with respect to the empty lattice energy bands are indicative of the effect of the crystal potential.

It will soon become apparent that shifts and splittings in the DBS, though quite noticeable, are not such as to make it look totally unlike the empty lattice dielectric band structure of Fig. 1. This explains why for many noncritical applications the usual diagonal $\epsilon(\vec{q})$ is sufficient.

The symmetries of the most screened eigenpotentials [i.e., those corresponding to the lowest $\epsilon_\nu^{-1}(\vec{q})$] reflect indirectly important characteristics of the underlying electronic structure, that is of the chemical bond in the crystal, as explained in Ref. 22. In Si and at $\vec{q}=0$ the most screened symmetries are, in order of increasing magnitude of $\epsilon_\nu^{-1}$, $\Gamma_2'$, $\Gamma_{15}$, $\Gamma_{25}'$, $\Gamma_{12}'$, $\Gamma_1$. The qualitative reason why a $\Gamma_2'$ perturbation is screened best, is because it excites transitions from bonding ($\Gamma_{25}'$) to antibonding ($\Gamma_{15}$) states most efficiently.

Another general fact worth noticing is that the (0, 0, 0) plane wave gives rise to a $\Gamma_1$ eigenpotential which is the lowest of all, and is also uncoupled to all the higher $\Gamma_1$'s. It is instead coupled to all higher $\Gamma_{15}$ eigenvalues, by the so-called

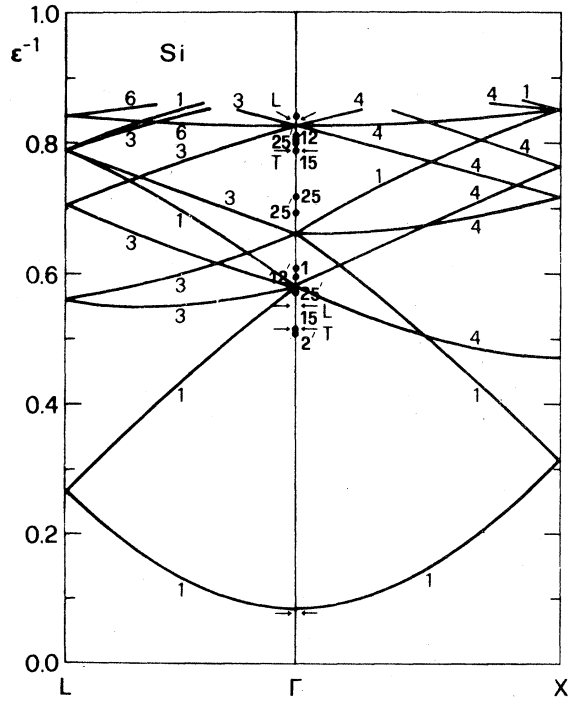


FIG. 1. "Empty lattice" dielectric band structure of silicon obtained by simple folding in the BZ of the diagonal $\epsilon^{-1}(\vec{q})$. The dots at Γ are the $\vec{q}\to 0$ accurate RPA results of Baldereschi and Tosatti (from Ref. 22).

"wings" of the DM, $\tilde{\epsilon}^{-1}(\vec{q},\vec{q}+\vec{G})$. For $\vec{q}\to 0$, these elements take the nonanalytic form $(\vec{q}/|\vec{q}|)\cdot\vec{C}(\vec{G})$. The coupling $\Gamma_1$–$\Gamma_{15}$ is at the origin of the "longitudinal-transverse splitting" of all $\Gamma_{15}$ eigenvalues ($\Gamma_{15}\to\Delta_1+\Delta_5$), for $\vec{q}\to 0$. Physically, what happens is that a longitudinal perturbation, even if cell-periodic, gives rise at long wavelength to a macroscopic field parallel to $\vec{q}$. This field, in turn, causes a response which is cell-periodic, and acts to reinforce the original perturbation, thus yielding a total reduction of screening power, i.e., an increase of $\epsilon_{\Delta_1}^{-1}(\vec{q}\to 0)$. The same does not happen for a transverse perturbation, whence the $L$–$T$ splitting, which is a completely analogous in nature to that well known for phonons.

We can now proceed to illustrate the DBS obtained with each of the models chosen.

### A. Sinha model

The DBS obtained by diagonalizing (3.1) is shown in Fig. 2. The dielectric bands are very few and very flat. Remarkably, only perturbations of symmetries $\Gamma_{25}'$ and $\Gamma_{15}$ ($=\Delta_1+\Delta_5$) at $\vec{q}=0$ are screened at all, while any other perturbation is left unscreened, including $\Gamma_2'$, which is known[22] to be in reality silicon's best screened. However, there are no $\vec{q}\to 0$ phonons in Si other than $\Gamma_{15}$ and $\Gamma_{25}'$, which shows that the model is practically custom made for use in lattice dynamics.[18,19] A general connection between DM factorizability and selective screening of a few symmetries only is elucidated in Appendix B.

The flatness of the dielectric bands of Fig. 2 indicates that Sinha's model leads to expect exceedingly large local-field effects, with strong deviations from purely diagonal screening. Comparison with either the accurate $\vec{q}=0$ eigenvalues of Fig. 1 or with other models discussed later in this section indicates that local-field effects are indeed overestimated in this model. This is not surprising, silicon being very far from a tight-binding two-band insulator, which is the ideal case where Sinha's model applies exactly.

### B. Johnson model

Not being factorizable, Johnson's DM strongly screens all symmetries and not just some of them. However, the DBS of Fig. 3 shows clearly that this is not a very good model either. A large number of bands are strongly compressed towards the lower values of $\epsilon^{-1}$. This means that the local-field effects, instead of becoming less and less important for higher bands (that is, for large $|\vec{G}|$ values), have an unphysical tendency to remain constant. For instance, the $L$–$T$ splittings at $\vec{q}\to 0$ remain of the same order

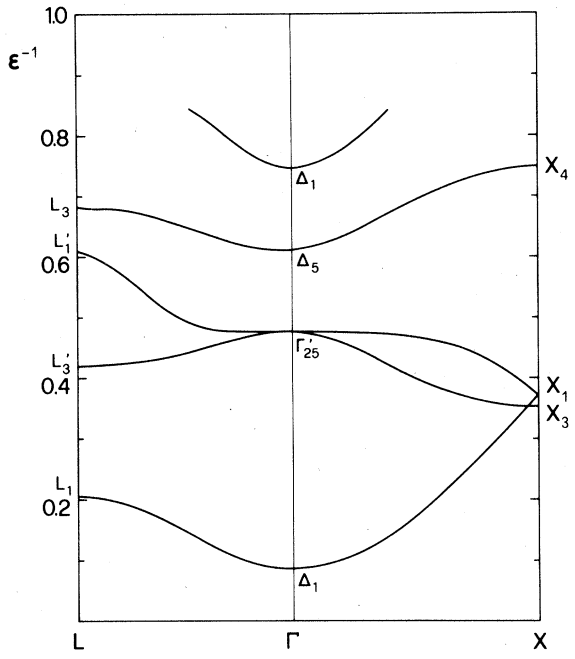


FIG. 2. Dielectric band structure of Si obtained with Sinha's model [Eq. (3.1)].

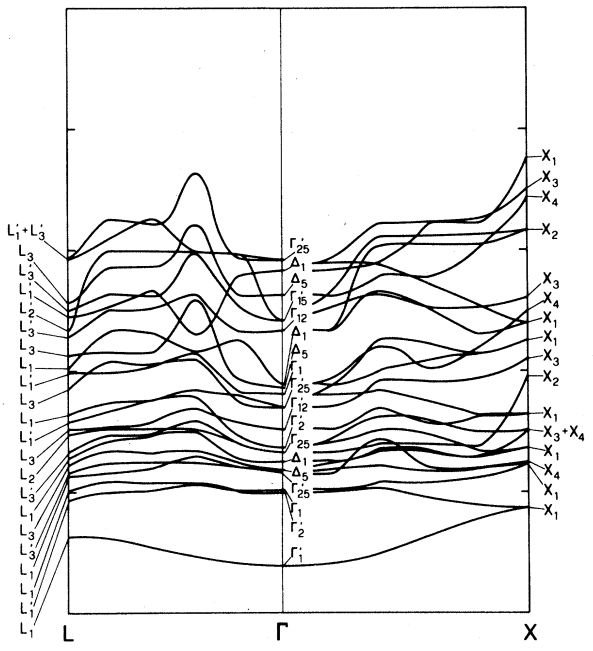


FIG. 3. Dielectric band structure of Si obtained with Johnson's model [Eq. (3.3)]. Vertical units are the same as in Fig. 2.

for higher as for lower bands, while they decrease strongly in the realistic calculation of Ref. 22. Furthermore, there are suspicious oscillations in the bands in the middle of the Brillouin zone which do not seem to have a proper physical motivation.

A closer inspection shows that the unphysical features just described are due to the cutoff $K$ introduced in the denominator for $|\vec{G}-\vec{G}'|>2k_F$. The large $L-T$ splittings are due to exceedingly large DM wings $\tilde{\epsilon}(\vec{q},\vec{q}+\vec{G})$, while the oscillations arise from the sudden onset of the cutoff $K$ in $\vec{q}$ space.

There is also another problem introduced by the cutoff, which is not directly shown on Fig. 3 in order not to make the figure too cumbersome but is nevertheless serious. At large $|\vec{q}+\vec{G}|$, where the diagonal DM elements are already very close to 1, the excessive magnitude of the off-diagonal elements leads to high-lying eigenvalues $\epsilon_\nu^{-1}(\vec{q})$ larger than 1. This is in contradiction with the general requirements of causality and thermodynamic stability (2.10). Thus Johnson's model describes a system that has a short-wavelength instability, unless care is taken to drop all the unphysical bands, $\epsilon_\nu^{-1}(\vec{q})>1$.

### C. Car-Selloni model

Clearly, once the cutoff is dropped, many of the undesirable features described above should disappear. The DBS corresponding to this model is shown in Fig. 4. By comparison with Fig. 1, we see that the eigenvalues have now quite reasonable

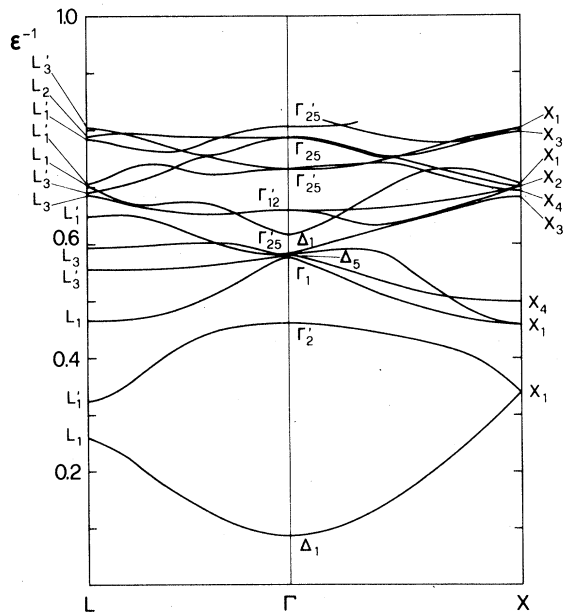


FIG. 4. Dielectric band structure of Si obtained with the Car-Selloni model [Eq. (3.5)].

magnitudes at the Γ point, and that they seem to retain a sensible behavior over all the BZ. The $L-T$ splitting also has the right order of magnitude, which is not surprising since the parameters in Eq. (3.5) are given the values that best fit the off-diagonal elements of the DM of Baldereschi and Tosatti.[22] However, although the most screened eigenvalues at Γ are the same as in Ref. 22, the ordering is not the same. We have found that it is not possible to reproduce this correct ordering with a formula like Eq. (3.5), neither by changing the values of the parameters $A$ and $B$, nor by slightly modifying the formula itself. We conclude that the simple local dependence on the valence charge density of Eq. (3.5), while quite good for a semiquantitative description of screening in Si—and, we would expect, other crystals as well—is not suitable when a high accuracy is required.

### D. Local-density model

The DBS obtained with the local-density (LD) model is presented in Fig. 5. The overall behavior is not very different from that of the Car-Selloni model, the deviations from the empty lattice bands being generally somewhat smaller. This indicates that a general tendency of the LD model may be to underestimate the local-field effects. All best screened symmetries at Γ are represented, though not always in the same order as in Ref. 22. However, the lowest $\Gamma_1$ eigenvalue is identically zero, and no $L-T$ splittings are found.

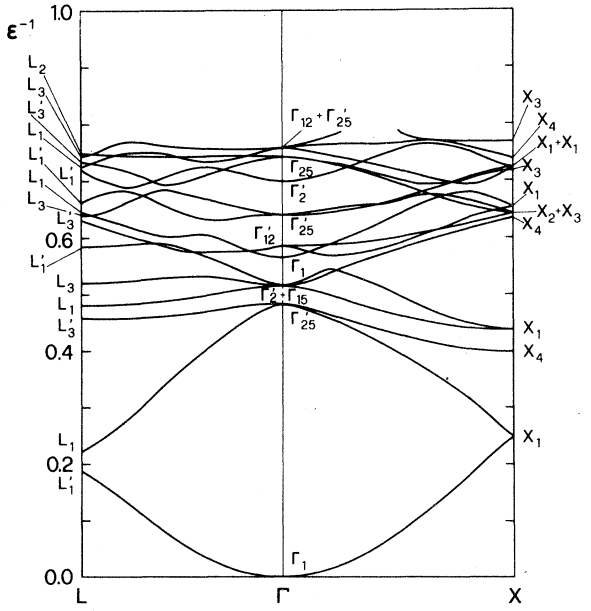


FIG. 5. Dielectric band structure of Si obtained with the local-density model [Eq. (3.6)].

This is a consequence of the fact, already mentioned in the Sec. IIID, that the LD formulation is not capable of giving a nonmetallic behavior in the dielectric response. Hence

$$\tilde{\epsilon}(\vec{q},\vec{q})\big|_{\vec{q}\to 0} \to q^{-2},$$
$$\tilde{\epsilon}(\vec{q},\vec{q}+\vec{G}) = \tilde{\epsilon}(\vec{q}+\vec{G},\vec{q}) \to q^{-1},$$

in this model, irrespective of the existence of a gap in the electronic spectrum.

In spite of this defect, this model seems to us quite an attractive one, both because it has a stronger theoretical basis than the others and because it is parameter-free, requiring the crystal density as its sole input. It can be of direct use to study screening in all those crystals where our knowledge has been so far very limited.

## V. AN APPLICATION: CHARGE INDUCED BY HIGH-SYMMETRY LATTICE VIBRATIONS

Though the dielectric band structure itself is a rather instructive object, it does not of course contain all the information of the full DM. The remaining part of information is contained in its eigenpotentials, which we have not discussed so far. A proper appraisal of the differences between DM models should include a comparison of their eigenpotentials. This is, however, both very cumbersome to do and rather devoid of immediate physical appeal. A more natural choice could be to compare, for example, real-space distributions of induced electronic charge when the crystal is subject to a given perturbation of practical occurrence. Examples of such perturbations could be a uniform external field,[28] point-charge impurity,[21,41] or a phononlike displacement of the atoms.[23] One extra bonus is that, in the lack of any direct experimental measurements, there exist accurate self-consistent calculations of these induced charges[23] against which the various models can be tested.

In this section we apply the different screening models discussed in the previous sections to the calculation of the induced charge caused by a high-symmetry lattice vibration in an Si crystal. The local charge distribution is, incidentally, a very relevant quantity to the microscopic theory of lattice vibrations, because the pointlike ion core feels the local field[42,43] rather than the mean field, such as one would calculate with a diagonal $\epsilon(\vec{q})$.

We have chosen the following two perturbations: (a) The unit cell of the distorted crystal contains two atoms, one at (000) and the other at $\frac{1}{4}a(111)(1+x)$. This corresponds for $x \neq 0$ to a $\Gamma_{25}'$ phonon displacement. (b) The distorted unit cell consists of four atoms at $(0,0,0)$, $\frac{1}{4}a(111)$, $\frac{1}{4}a(2+x,x,2)$, and $\frac{1}{4}a(3+x,1+x,3)$. This corresponds to an $X_3$

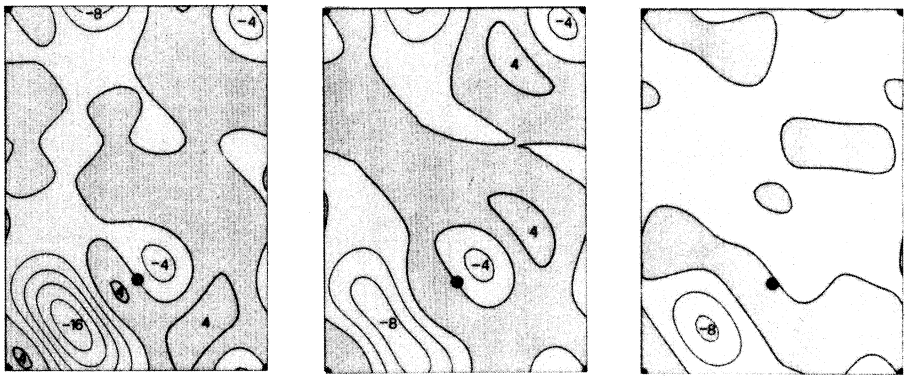


FIG. 6. Accurate results (from Ref. 23) for the induced electron charge density (in units of 0.01 electrons per cell) produced in the $(1\bar{1}0)$ plane by the $\Gamma_{25}'$ distortion described in the text with $x=0.004$. (a) Total induced charge; (b) diagonal contribution; (c) off-diagonal contribution.

phonon displacement.

The reason for this choice is because Baldereschi and Maschke[23] provided a self-consistent pseudopotential calculation of the charge-density change for these displacements of the atoms for small $x$. Figures 6 and 7 show their results, plotted as constant density contours in the Si unit cell. These authors have shown, furthermore, that the charge induced via linear screening by a $\Gamma_{25}'$ phonon displacement, defined in terms of the bare atomic pseudopotential $v^{\text{at}}$ as

$$\rho^{\text{ind}}(\vec{r})=\sum_{\vec{G}\vec{G}'}\exp(i\vec{G}\cdot\vec{r})v^{-1}(\vec{G})[\epsilon^{-1}(\vec{G},\vec{G}')-\delta_{\vec{G}\vec{G}'}]V_{\vec{G}'}^{25'}, \tag{5.1}$$

where

$$V_{\vec{G}}^{25'}=\int d^3r\, e^{-i\vec{G}\cdot\vec{r}}\sum_{\vec{R}}[v^{\text{at}}(\vec{R}+\vec{d}(x)-\vec{r})-v^{\text{at}}(\vec{R}+\vec{d}(0))] \tag{5.2}$$

is, if $\epsilon^{-1}$ is the DM of Ref. 11, almost indistinguishable from that obtained directly by difference between two full self-consistent pseudopotential calculations. No such comparison had been possible for the $X_3$ phonon, as there was no DM calculation at $X$. However, since the diagonal dielectric function $\epsilon(\vec{q})$ is well known at all $\vec{q}$ in Si,[33] it is possible to separate the diagonal and the off-diagonal contributions to the total screening charge, both at $\Gamma$ and at $X$. The separate contributions to the screening charge found in this way by Baldereschi and Maschke are plotted in Figs. 6(b), 6(c), 7(b), and 7(c).

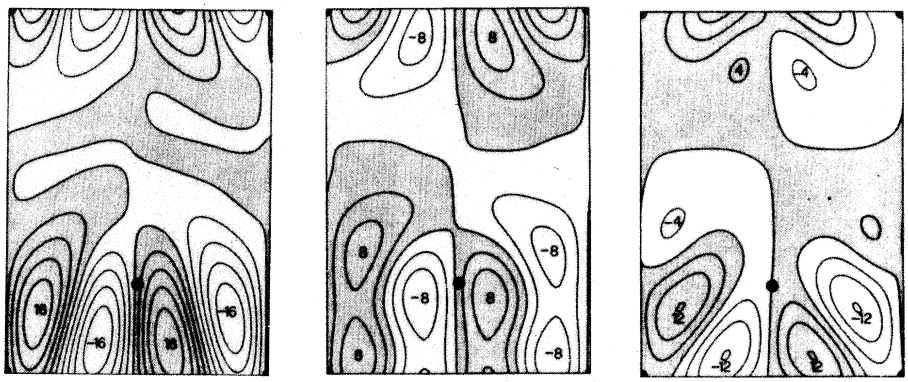


FIG. 7. Accurate results (from Ref. 23) for the induced electron charge density (in units of 0.1 electrons per cell) produced in the $(1\bar{1}0)$ plane by the $X_3$ distortion described in the text with $x=0.1$. (a) Total induced charge; (b) diagonal contribution; (c) off-diagonal contribution.

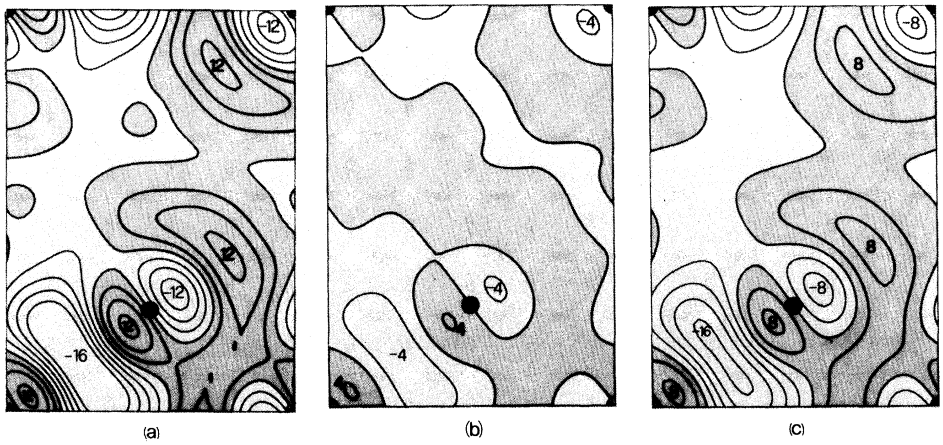


FIG. 8. Induced electron charge density in Si (in units of 0.01 electron per cell) obtained with Sinha's DM model in the $(1\bar{1}0)$ plane by the $\Gamma'_{25}$ distortion described in the text with $x=0.004$. (a) Total induced charge; (b) diagonal contribution; (c) off-diagonal contribution.

We have calculated the induced charge (5.1) for the $\Gamma'_{25}$ phonon, and that, defined similarly, for the $X_3$ phonon, by using the DM models described in the previous sections. The bare pseudopotential $v^{\text{at}}(\vec{r})$ has been chosen to be the same as that of Baldereschi and Maschke,[44] and also the distortion magnitudes $x$ are the same. The results of the Sinha, Car-Selloni, and local-density models are presented for comparison with the full calculations, in Figs. 8–13. (Johnson's model has been omitted now, on account of its many unphysical features.)

The following comments can be made. It is known that, while the diagonal screening gives rise to dipoles centered on the atoms, the off-diagonal screening in the diamond structure gives rise to additional dipoles centered on the bonds.[45,28,23] For a $\Gamma'_{25}$ perturbation, which is itself parallel to the bond, the atom and bond dipoles are lined up, that is, the off-diagonal screening merely reinforces the diagonal effect. In an $X_3$ perturbation, instead, the atom and the bond screening keep their individuality. The relative importance of the bond contribution is larger, with the bond screening charge oriented differently from the atomic screening charge. This contrasting behavior can be seen by comparing Figs. 6 and 7.

The results for the Sinha model, Figs. 8 and 9, indicate a tendency to overestimate the off-diagonal screening, that is the magnitude of the bond dipole, which has become even more important than the diagonal. A second fact is that the bond dipole lines up with the atom dipole not only in the

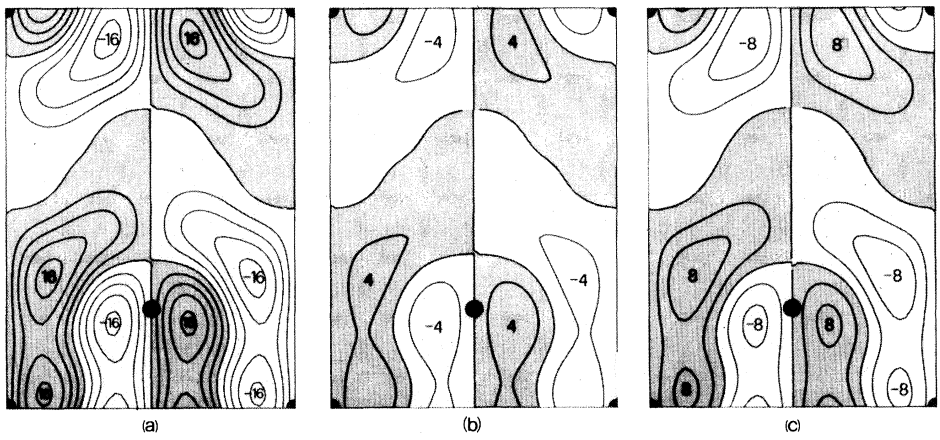


FIG. 9. Induced electron charge density in Si (in units of 0.1 electrons per cell) obtained with Sinha's DM model in the $(1\bar{1}0)$ plane by the $X_3$ distortion described in the text, with $x=0.1$. (a) Total induced charge; (b) diagonal contribution; (c) off-diagonal contribution.

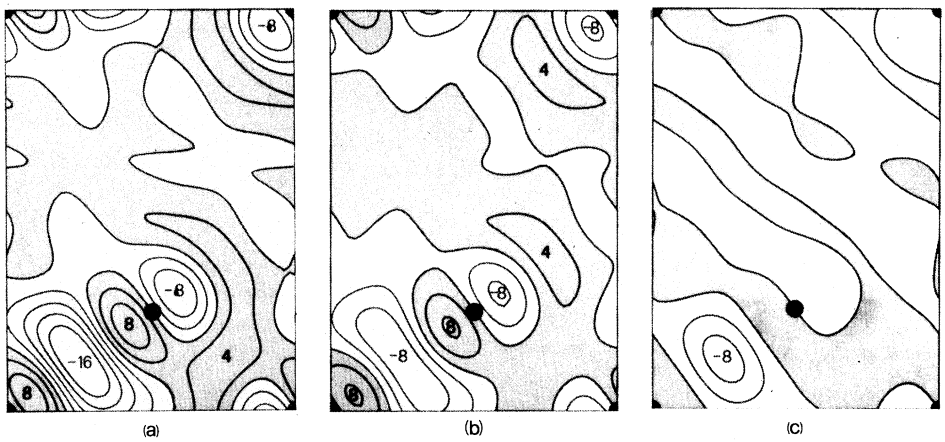


FIG. 10. Same as Fig. 8 with the Car-Selloni DM.

$\Gamma'_{25}$ case, but also in the $X_3$ case, contrary to the self-consistent results.

The Car-Selloni model gives, of course, good results for a $\Gamma'_{25}$ perturbation (Fig. 10), with off-diagonal effects practically indistinguishable from those of Fig. 6. However, the bond dipoles are somewhat underestimated for the $X_3$ perturbation (Fig. 11), and their direction is intermediate between parallel and transverse to the bond direction, while the full calculation indicates a rather more transverse direction.

Finally, the local-density model exhibits a screening charge of qualitative features similar to those of the full calculation, both for $\Gamma'_{25}$ (Fig. 12) and $X_3$ perturbations (Fig. 13). Quantitatively, however, there is a general tendency to underestimate local-field effects (that is, the bond dipoles are smaller than they should be) both with respect to the full calculation and with respect to the Car-Selloni model.

Summing up, the above comparison of induced charge densities leads to fairly similar conclusions to those based on comparing dielectric band structures: Local-field effects in Si are too strong and lack symmetry in Sinha's model and are substantially better represented but somewhat weaker than they should be in the Car-Selloni and local-density models.

## VI. CONCLUSIONS

In this work we have addressed the general problem of electronic screening in a crystal and further developed the dielectric band-structure approach to handle it. The extension of the general properties of causality and thermodynamic stability to this case shows that all inverse dielectric eigenvalues must be smaller than one, but not necessarily positive. Continuous electronic phase transitions occur, in particular, when one inverse dielectric eigenvalue goes to $-\infty$.

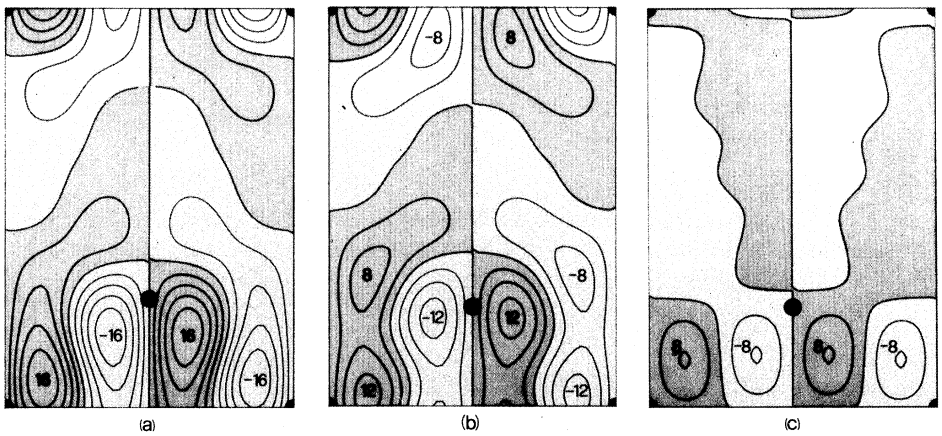


FIG. 11. Same as Fig. 9 with the Car-Selloni DM.

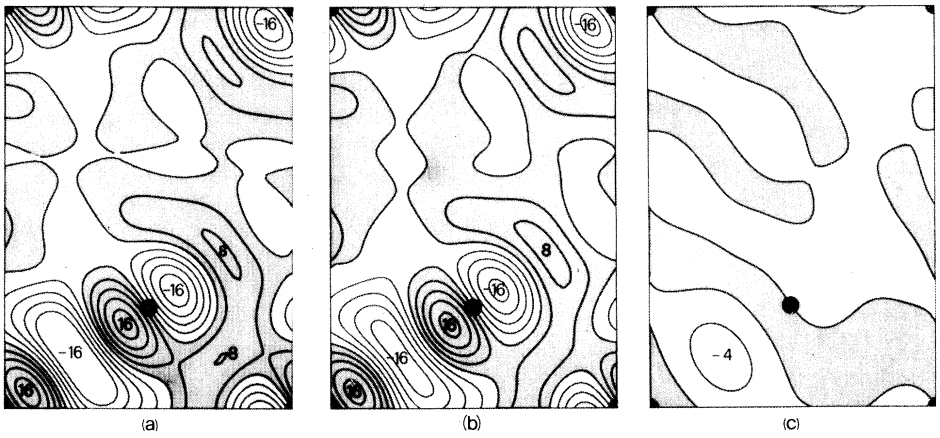


FIG. 12. Same as Fig. 8 with the local-density model.

The problem of a full dielectric band-structure calculation throughout the Brillouin zone is then considered, for the test case of silicon, which is the crystal whose dielectric properties are best known. Four different dielectric matrix models are considered, among those existing in literature: They are the models of Sinha, Johnson, Car and Selloni, and a newly developed one based on a local-density functional. Comparison among their dielectric bands, and with those calculated by Baldereschi and Tosatti at $\vec{q} \to 0$ leads to the conclusion that local-field effects are generally overestimated by the models of Sinha and Johnson models, while they are underestimated, but generally better represented, by the Car-Selloni and the local-density models. Also, the important general fact that factorizable models necessarily screen only perturbations of a small incomplete set of symmetries is brought out. It is also found that certain dielectric matrices, such as Johnson's, violate either causality or stability, and must be dropped.

To compensate for the fact that no direct comparison with experiment is possible at this stage, we have calculated with linear response the induced charge densities for periodic phononlike $\Gamma_{25}$ and $X_3$ displacements of the atoms and compared the results with the full self-consistent pseudopotential calculations of Baldereschi and Maschke.[23] The extent to which the two approaches agree varies substantially from one model to another. Conclusions that can be drawn this way support strongly those obtained by simple comparison of dielectric bands.

## ACKNOWLEDGMENTS

The authors would like to thank Professor Abdus Salam and Professor Paolo Budini, the International Atomic Energy Agency, and UNESCO for hospitality at the International Centre for Theo-

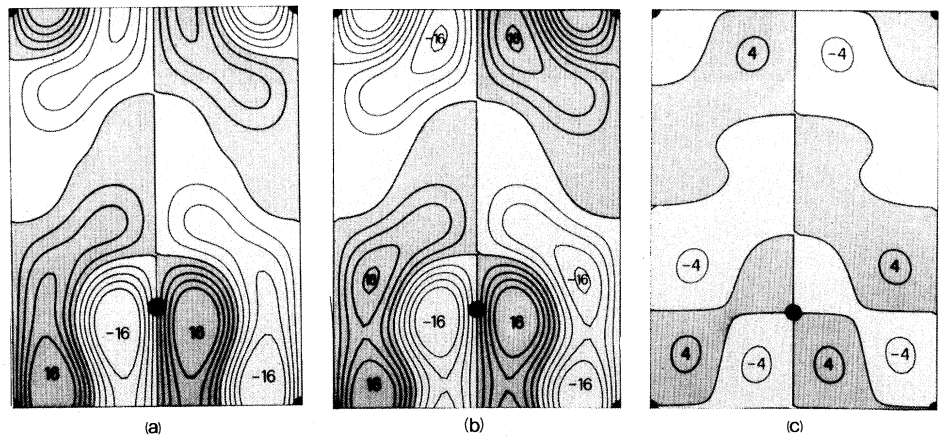


FIG. 13. Same as Fig. 9 with the local-density model.

retical Physics, Trieste and at the Scuola Internationale Superiore di Studi Avanzati, Trieste. They also wish to thank K. Maschke for stimulating discussions and for his help with the phonon charge calculation, and A. Baldereschi for useful discussions. A special acknowledgment is due to Annabella Selloni, who cooperated with us in the earliest stages of this work.

## APPENDIX A: DENSITY-FUNCTIONAL DIELECTRIC MATRIX

According to the theorem of Hohenberg and Kohn,[46] the ground-state energy of a system of $N$ interacting electrons in the external (local) field $V(\vec{r})$ is a unique functional of the electron charge density, which can be written in the form

$$E_V[\rho] = \int d^3r\, V(\vec{r})\rho(\vec{r}) + \tfrac{1}{2}\int \frac{\rho(\vec{r})\rho(\vec{r}')}{|\vec{r}-\vec{r}'|}\, d^3r\, d^3r' + G[\rho], \tag{A1}$$

where $G[\rho]$ is a universal functional of $\rho(\vec{r})$ that includes kinetic and exchange-correlation contributions to the total energy. From the minimum property of (A1) subject to the condition $\int \rho(\vec{r})d^3r = N$ we get

$$\frac{\delta E_V[\rho]}{\delta\rho(r)} - \mu = 0, \tag{A2}$$

i.e.,

$$V_{sc}(\vec{r}) = V(\vec{r}) + \phi(\vec{r}) - \mu = -\frac{\delta G[\rho]}{\delta\rho(\vec{r})}. \tag{A3}$$

Here $\mu$ is the chemical potential and

$$\phi(\vec{r}) = \int \frac{\rho(\vec{r}')}{|\vec{r}-\vec{r}'|}\, d^3r'.$$

The left-hand side term of Eq. (A3) has the meaning of the self-consistent field $V_{sc}(\vec{r})$ seen by a test charge in the system.

By taking the functional derivative of Eq. (A3) with respect to $\rho(\vec{r})$ we get the response function

$$R(\vec{r},\vec{r}') = \frac{\delta V_{sc}(\vec{r})}{\delta\rho(\vec{r}')} = -\frac{\delta^2 G[\rho]}{\delta\rho(\vec{r})\delta\rho(\vec{r}')} \tag{A4}$$

or in Fourier space

$$R(\vec{q}+\vec{G},\vec{q}+\vec{G}') = -\frac{\delta^2 G[\rho]}{\delta\rho_{\vec{q}+\vec{G}}\delta\rho_{-(\vec{q}+\vec{G}')}}, \tag{A5}$$

where $\rho_{\vec{Q}}$ are Fourier components of the charge density. The DM is given by

$$\epsilon(\vec{q}+\vec{G},\vec{q}+\vec{G}') = \delta_{\vec{G}\vec{G}'} + v(\vec{q}+\vec{G})\tilde{\chi}(\vec{q}+\vec{G},\vec{q}+\vec{G}') \tag{A6}$$

in terms of the density response

$$\tilde{\chi}(\vec{q}+\vec{G},\vec{q}+\vec{G}') = -\frac{\delta\rho_{\vec{q}+\vec{G}}}{\delta V_{sc}(-\vec{q}-\vec{G}')} = -R^{-1}(\vec{q}+\vec{G},\vec{q}+\vec{G}'). \tag{A7}$$

We get, therefore, Eq. (3.6) with $R$ given by Eq. (A7).

This formulation is exact and completely general: From the knowledge of the functional $G[\rho]$ and of the equilibrium charge density which satisfies Eq. (A3) we can calculate $R$, whose inverse gives the proper polarization part $\tilde{\chi}$. In practice, however, we must content ourselves with an approximate form of $G[\rho]$. In the present paper we have chosen the Thomas-Fermi local form corrected with first gradients[47]:

$$G[\rho] = c_0\int d^3r\, \rho^{5/3}(\vec{r}) + c_1\int d^3r \frac{|\vec{\nabla}\rho(\vec{r})|^2}{\rho(\vec{r})} \tag{A8}$$

from which Eq. (3.7) follows directly. The form (A8) does not include exchange and correlation effects, and is appropriate to the comparison with the RPA results of Baldereschi and Tosatti.[11]

In our application we do not use in Eq. (3.7) the equilibrium charge density obtained with Eq. (A3) with the functional (A8), but simply use in Eq. (3.7) the empirical pseudopotential charge density. This is a common practice in Thomas-Fermi methods. Indeed it is known[47] that the Thomas-Fermi approximation with gradient corrections can badly fail in some applications when used as a variational method, but gives in any case a fairly accurate approximation of the total energy if an accurate charge density (Hartree-Fock, pseudopotential, experimental, etc.) is used as an input to the Thomas-Fermi formulas.

A more complete account of this density-functional based method will be given in a future publication.[32] It should be pointed out, in closing, that a complete self-consistent formulation of the local-density linear screening theory in real space has been given previously by Ying, Smith, and Kohn,[48] who applied it to the problem of chemisorption from jellium surfaces.

## APPENDIX B: SYMMETRY ANALYSIS OF FACTORIZABLE DM MODELS

The fact that only a few specific symmetries are screened in Sinha's model is a direct consequence of the factorizable nature of that model. To see this more clearly let us set $\epsilon_0(\vec{q}+\vec{G}) = 1$ in Eq. (3.1) and look in detail at the part of the Sinha DM that is responsible for LF effects, i.e., to

$$\tilde{\epsilon}(\vec{q}+\vec{G},\vec{q}+\vec{G}') - \delta_{\vec{G}\vec{G}'} = [v'(\vec{q}+\vec{G})v'(\vec{q}+\vec{G}')]^{1/2} \times \tilde{\chi}(\vec{q}+\vec{G},\vec{q}+\vec{G}'), \tag{B1}$$

where

$$\tilde{\chi}(\vec{q}+\vec{G},\vec{q}+\vec{G}') = a_0(\vec{q}+\vec{G})\cdot(\vec{q}+\vec{G}') \times f^*(\vec{q}+\vec{G})f(\vec{q}+\vec{G}')\sum_s e^{i(\vec{G}-\vec{G}')\cdot\vec{\tau}_s} \tag{B2}$$

We can restrict our analysis to the $\Gamma$ point and consider only the matrix (B1) at $\vec{q}=0$,[49] in order to avoid the complication of the DM nonanalyticity in the limit $\vec{q}\to 0$. This is equivalent to consider the DM without the wings, i.e., without the first row and the first column. Considering the complete matrix for $\vec{q}\to 0$ will only cause $L-T$ splittings of the $\Gamma_{15}$ eigenvalues found for $\vec{q}=0$.[22]

We note first, by inspection of Eq. (B1), that the symmetry of the eigenvalues of $\tilde{\epsilon}(\vec{G},\vec{G}')$ is the same as that of the eigenvalues of $\tilde{\chi}(\vec{G},\vec{G}')$. Therefore in the following we will concentrate on the "polarization matrix" $\tilde{\chi}$. We also switch to a real-space representation, which is more appropriate to this discussion. The matrix $\tilde{\chi}(\vec{r},\vec{r}')$ is given in the RPA by[50]

$$\tilde{\chi}(\vec{r},\vec{r}')=2\sum_{ij}\frac{f_i-f_j}{E_i-E_j}\psi_i(\vec{r})\psi_j^*(\vec{r})\psi_i(\vec{r}')\psi_j(\vec{r}')\,, \tag{B3}$$

where the sums run over all the states $i$ in the crystal and the $f_i$'s are Fermi occupation numbers.

We expand the wave functions $\psi_i(\vec{r})$ in terms of localized Wannier functions $\phi_{n\lambda}(r)$,

$$\psi_i(\vec{r})=\frac{1}{\sqrt{N}}\sum_{\lambda,\vec{R}} e^{i\vec{k}\cdot\vec{R}}C_{n\lambda}(\vec{k})\varphi_{n\lambda}(\vec{r}-\vec{R})\,. \tag{B4}$$

Here $n$ is a band index, $\vec{k}$ is the reduced momentum, $\lambda$ is a site in the cell $\vec{R}$, and $N$ is the number of cells. Substituting (B4) into (B3)

$$\tilde{\chi}(\vec{r},\vec{r}')=\sum_{ij}\frac{2}{N^2}\frac{f_i-f_j}{E_i-E_j}\sum_{\substack{\vec{R}_1\vec{R}_2\vec{R}_3\vec{R}_4\\ \lambda_1\lambda_2\lambda_3\lambda_4}}\exp[i\vec{k}_i(\vec{R}_1-\vec{R}_2)+i\vec{k}_j\cdot(\vec{R}_4-\vec{R}_2)]\,C_{n_i\lambda_1}(\vec{k}_i)C^*_{n_j\lambda_2}(\vec{k}_j)C^*_{n_i\lambda_3}(\vec{k}_i)C_{n_j\lambda_4}(\vec{k}_j)$$
$$\times\phi_{n_i\lambda_1}(\vec{r}-\vec{R}_1)\phi^*_{n_j\lambda_2}(\vec{r}-\vec{R}_2)\phi^*_{n_i\lambda_3}(\vec{r}-\vec{R}_3)\phi_{n_j\lambda_4}(\vec{r}-\vec{R}_4)\,. \tag{B5}$$

If we now restrict to a two-band model, with tightly bound flat bands, the product of two Wannier functions is different from zero only if both belong to the same unit cell and the same site. We obtain, like Ortuno and Inkson,[14]

$$\tilde{\chi}(\vec{r},\vec{r}')=\frac{4}{E_g}\sum_{\lambda,\vec{R}}A_\lambda(\vec{r}\cdot\vec{R})A^*_\lambda(\vec{r}'-\vec{R})\,, \tag{B6}$$

where

$$A_\lambda(\vec{r}-\vec{R})=\varphi_{\mathrm{cond},\lambda}(\vec{r}-\vec{R})\varphi^*_{\mathrm{val},\lambda}(\vec{r}-\vec{R})\,. \tag{B7}$$

One recovers Sinha's model (B1) from (B6) if the sites $\lambda$ are the atomic sites $s$ and the conduction and valence Wannier functions are $p$- and $s$-like, respectively.[51] On the other hand, if the sites $\lambda$ are the bond sites and $\varphi_{\mathrm{val}}$, $\varphi_{\mathrm{cond}}$ are bonding and antibonding combinations of $sp^3$ hybrids, one obtains another popular form of the extreme-tight-binding model, namely, the model used by Ortuno and Inkson,[14] Turner and Inkson,[15] and Arya and Jha.[17] From (B7) and the assumption of two flat bands, it follows that

$$\int A_\lambda(\vec{r}-\vec{R})A^*_{\lambda'}(\vec{r}-\vec{R}')d^3r$$
$$=\delta_{\lambda\lambda'}\delta_{\vec{R}\vec{R}'}\int\varphi_{\mathrm{cond},\lambda}(\vec{r})\varphi^*_{\mathrm{cond},\lambda}(\vec{r})\varphi^*_{\mathrm{val},\lambda}(\vec{r})\varphi_{\mathrm{val},\lambda}(\vec{r})d^3r\,. \tag{B8}$$

This means that the matrix (B6) is a real-space representation of the operator

$$\hat{\chi}=\frac{4}{E_g}\sum_{\lambda,\vec{R}}|A_{\lambda\vec{R}}\rangle\langle A_{\lambda\vec{R}}|\,, \tag{B9}$$

i.e., a sum of projection operators over the states $|A_{\lambda\vec{R}}\rangle$. The eigenvectors of (B9) having Bloch character are, for $\vec{q}=0$,

$$|\phi_\lambda^{\vec{q}=0}\rangle=\sum_{\vec{R}}|A_{\lambda\vec{R}}\rangle\,. \tag{B10}$$

The number of different sites in the unit cell times the possible degeneracy of state $A_\lambda$ gives, therefore, the total number of eigenvalues of the operator (B9). Of course, some of these eigenvalues can be degenerate.

In the case of Sinha's model we have two atomic sites in the unit cell and the localized functions $A_{\lambda\vec{R}}$ have $\vec{p}$ character. The corresponding symmetrized combinations of Bloch sums can have $\Gamma_{15}$ and $\Gamma'_{25}$ symmetries; hence Sinha's DM model can have only two eigenvalues different from 1, corresponding to these two symmetries, $\Gamma_{15}$ and $\Gamma'_{25}$. The addition of the DM wings in the case $\vec{q}\to 0$ introduces the $L-T$ splitting of the $\Gamma_{15}$ eigenvalue into $\Delta_1$ and $\Delta_5$ as can be seen in Fig. 2. In the same figure there are also other eigenvalues close to 1 but not exactly 1 due to the artificial addition of the homogeneous screening term $\epsilon_0(Q)$.

The same symmetry analysis can be applied to the extreme tight-binding model based on Wannier functions localized at the bonds.[14,15] One obtains for this model only eigenvalues of symmetry $\Gamma'_2$ and $\Gamma_{15}$ at $\vec{q}=0$, which become $\Gamma'_2$ and $\Delta_1+\Delta_5$ in the limit $\vec{q}\to 0$. This model has been extensively applied to phonons,[15,16] giving rise to reasonable dispersion curves. However, since it does not contain the symmetry $\Gamma'_{25}$, which is the symmetry of the optical phonon at $\Gamma$ in covalent semicon-

ductors with the diamond structure, the induced electronic charge due to a $\Gamma'_{25}$ lattice distortion is exactly zero in this model. We conclude, therefore, that even if the phonon frequencies obtained at $\Gamma$ with this model are numerically good, the microscopic field behind them is certainly misrepresented by this type of DM.

---

*Address during 1981: IBM Research Laboratories, Yorktown Heights, New York 10598.
†Permanent address.

[1]P. C. Martin and J. Schwinger, Phys. Rev. 115, 1342 (1959).
[2]S. L. Adler, Phys. Rev. 126, 413 (1962); N. Wiser, *ibid.* 129, 62 (1963).
[3]A. Baldereschi, Phys. Rev. B 7, 5212 (1973); D. J. Chadi and M. L. Cohen, *ibid.* 12, 5747 (1973).
[4]J. T. Devreese, P. E. Van Camp, and V. E. Van Doren, Phys. Rev. Lett. 42, 1224 (1979).
[5]J. A. Van Vechten and R. M. Martin, Phys. Rev. Lett. 28, 446 (1972).
[6]W. Hanke and L. J. Sham, Phys. Rev. Lett. 33, 582 (1974).
[7]N. E. Brener, Phys. Rev. B 12, 1487 (1975).
[8]S. P. Singhal, Phys. Rev. B 12, 564 (1975).
[9]S. G. Louie, J. R. Chelikowsky, and M. L. Cohen, Phys. Rev. Lett. 34, 155 (1975).
[10]J. T. Devreese, P. E. Van Camp, and V. E. Doren, Bull. Am. Phys. Soc. 23, 224 (1978).
[11]A. Baldereschi and E. Tosatti, Phys. Rev. B 17, 4710 (1978).
[12]C. M. Bertoni, V. Bortolani, C. Calandra, and E. Tosatti, Phys. Rev. B 9, 1710 (1974).
[13]J. C. Inkson, J. Phys. C 7, 1571 (1974).
[14]M. Ortuno and J. C. Inkson, J. Phys. C 12, 1065 (1979).
[15]R. D. Turner and J. C. Inkson, J. Phys. C 11, 2875 (1978).
[16]L. E. Oliveira and M. Ortuno, Solid State Commun. 33, 821 (1980).
[17]K. Arya and S. S. Jha, Phys. Rev. B 9, 4485 (1974).
[18]S. K. Sinha, Phys. Rev. 177, 1256 (1969).
[19]S. K. Sinha, R. P. Gupta, and D. L. Price, Phys. Rev. B 9, 2564 (1974); 9, 2573 (1974).
[20]D. L. Johnson, Phys. Rev. B 9, 4475 (1974).
[21]R. Car and A. Selloni, Phys. Rev. Lett. 40, 1365 (1979).
[22]A. Baldereschi and E. Tosatti, Solid State Commun. 29, 131 (1979).
[23]A. Baldereschi and K. Maschke, in *Proceedings of the International Conference on Lattice Dynamics*, edited by M. Balkanski (Flammarion, Paris, 1978), p. 36; and in *Proceedings of the International Conference on the Physics of Semiconductors, Edinburgh, 1978,* edited by B. L. H. Wilson (Institute of Physics, Bristol, 1978), p. 673.
[24]P. C. Martin, Phys. Rev. 161, 143 (1967).
[25]D. A. Kirzhnits, Usp. Fiz. Nauk 119, 357 (1976) [Sov. Phys.-Usp. 19, 530 (1976)]; O. V. Dolgov, D. A. Kirzhnits, E. G. Maksimov, Rev. Mod. Phys. 53, 81 (1981).
[26]A. Fasolino, M. Parrinello, and M. P. Tosi, Phys. Lett. 66A, 119 (1978).
[27]M. H. Cohen and H. Ehrenreich, Phys. Rev. 115, 786 (1959).
[28]A. Baldereschi, R. Car, and E. Tosatti, Solid State Commun. 32, 757 (1979).
[29]P. W. Anderson, in *Proceedings of All-Union Conference on the Physics of Dielectrics* (USSR Academy of Sciences, Moscow, 1958), p. 290; W. Cochran, Adv. Phys. 9, 387 (1960).
[30]W. Kohn, in *Many Body Physics*, edited by R. Balian (Gordon and Breach, New York, 1967), p. 355.
[31]G. F. Giuliani, E. Tosatti, and M. P. Tosi, J. Phys. C 12, 2769 (1979).
[32]S. Baroni, R. Car, and E. Tosatti (unpublished).
[33]J. P. Walter and M. L. Cohen, Phys. Rev. B 2, 1821 (1970).
[34]Actually this form applies only to the screening of the "electron-nonelectron" interaction as discussed, e.g., by L. Kleinman [Phys. Rev. 160, 585 (1967); 172, 383 (1968)], by L. Ballentine [Phys. Rev. 158, 670 (1967)], and also by V. Heine and D. Weaire [in *Solid State Physics*, edited by F. Seitz, D. Turnbull, and H. Ehrenreich (Academic, New York, 1974), Vol. 24]. It should be noted that all other models discussed here refer instead to screening of a "nonelectron-nonelectron" interaction.
[35]K. S. Singwi, A. Sjoländer, M. P. Tosi, and R. H. Land, Phys. Rev. B 1, 1044 (1970).
[36]W. Hanke and L. J. Sham, Phys. Rev. B 12, 4501 (1975).
[37]P. V. Giaquinta, M. Parrinello, E. Tosatti, and M. P. Tosi, J. Phys. C 9, 2031 (1976).
[38]D. R. Penn, Phys. Rev. 128, 2093 (1962).
[39]In our calculation we use the local pseudopotential form factors defined for Si by M. L. Cohen and J. Chelikowsky, Phys. Rev. B 10, 5095 (1974).
[40]R. Car and A. Selloni (unpublished).
[41]V. E. Godwin and E. Tosatti, Nuovo Cimento 54B, 497 (1979).
[42]L. J. Sham, Phys. Rev. 188, 1431 (1969).
[43]R. M. Pick, M. H. Cohen, and R. M. Martin, Phys. Rev. B 1, 910 (1970).
[44]Baldereschi and Maschke used in their calculation the bare pseudopotential $Si^{4+}$ of J. Appelbaum and D. R. Hamann, Phys. Rev. B 8, 1777 (1973).
[45]E. Tosatti, C. M. Bertoni, V. Bortolani, and C. Calandra, J. Phys. C 5, L299 (1972).
[46]P. Hohenberg and W. Kohn, Phys. Rev. 136, B864 (1964).
[47]See, for instance, N. H. March, Adv. Phys. 6, 1 (1957).
[48]S. C. Ying, J. R. Smith, and W. Kohn, Phys. Rev. B 11, 1483 (1975).
[49]We recall that gauge invariance implies that $\tilde{\epsilon}(0,0) = \tilde{\epsilon}(0,\vec{G}) = 0$ (see Refs. 11 and 22).
[50]See, for instance, L. Hedin and S. Lundquist, in *Solid State Physics*, edited by F. Seitz, D. Turnbull, and H. Ehrenreich (Academic, New York, 1969), Vol. 23.
[51]In this case $\lambda$ is a composite index standing for the site and the $x, y, z$ character of the conduction state.